

CHAPTER 25

RECENT DEVELOPMENTS IN THE STUDY OF BREAKING WAVES

by

Michael S. Longuet-Higgins
Royal Society Research Professor
Department of Applied Mathematics and Theoretical
Physics, Cambridge, England and Institute of
Oceanographic Sciences, Wormley, Godalming, Surrey

1. INTRODUCTION

The sight and sound of breaking waves and surf is so familiar and enjoyable that we tend to forget how little we really understand about them. Why is it, that compared to other branches of wave studies our knowledge of breaking waves is so empirical and inexact?

The reason must lie partly in the difficulty of finding a precise mathematical description of a fluid flow that is in general nonlinear and time-dependent. The fluid accelerations can no longer be assumed to be small compared to gravity, as in Stokes's theory for periodic waves and the theory of cnoidal waves in shallow water, nor is the particle velocity any longer small compared to the phase velocity.

The aim of this paper is to bring together some recent contributions to the calculation both of steep symmetric waves and of time-dependent surface waves. These have a bearing on the behaviour of whitecaps in deep water and of surf in the breaker zone.

Since spilling breakers in gently shoaling water closely resemble solitary waves, we begin with the description of solitary waves of limiting amplitude, then discuss steep waves of arbitrary height. The observed intermittency of whitecaps is discussed in terms of the energy maximum, as a function of wave steepness. In Sections 6 and 7 a simpler description of steady symmetric waves is proposed, using an asymptotic expression for the flow near the wave crest. Finally we describe a new numerical technique (MEL, or mixed Eulerian-Lagrangian) with which it has been found possible to follow the development of periodic waves past the point when overturning takes place.

2. THE LIMITING SOLITARY WAVE

A simple and very accurate approximation to the limiting solitary wave has recently been given by Longuet-Higgins (1974). If x and y are horizontal and vertical coordinates and h the undisturbed depth of water, then the surface profile on one side ($x > 0$) is approximated by

$$y/h = Ae^{-\lambda x/h} + Be^{-\mu x/h} \quad (2.1)$$

The constants A , B and λ , μ are determined by the conditions, first, that the particle at the crest moves with the phase-speed $c = F\sqrt{gh}$. So from Bernoulli's equation,

$$y/h = \frac{1}{2}F^2 \quad (x = 0), \quad (2.2)$$

Secondly, the angle of inclination at the surface is -30° , so

$$dy/dx = -1/\sqrt{3} \quad (x = 0). \quad (2.3)$$

We know thirdly (see Lamb, 1932 § 252), that in the outer fringes of the wave ($x \rightarrow \infty$) the profile behaves asymptotically like $e^{-\lambda x}$, where

$$\frac{\tan \lambda}{\lambda} = F^2 \tag{2.4}$$

exactly. This is satisfied by (2.0) if $0 < \lambda < \mu$. Fourthly we have Starr's exact relation

$$3V/g = (F^2 - 1) M \tag{2.5}$$

where V is the potential energy and M the mass:

$$V/g = \int_{-\infty}^{\infty} \frac{1}{2} y^2 dx, \quad M = \int_{-\infty}^{\infty} y dx;$$

and lastly an exact relation

$$\int_{-\infty}^{\infty} [(1 + y/h)(1 - 2F^{-2}y/h)^{1/2}(1 + dy/dx^2)^{1/2} - 1] dx = 0 \tag{2.6}$$

proved by Longuet-Higgins (1974). Equations (2.2) to (2.6) are five relations to determine the constants A, B, λ, μ and F , giving

$$\left. \begin{aligned} A &= 1.5389, & \lambda &= 1.0495 \\ B &= -.7093, & \mu &= 1.4630 \\ F^2 &= 1.6592. \end{aligned} \right\} \tag{2.7}$$

The resulting profile, plotted in Figure 1, agrees numerically with that given by Yamada (1957) to within 1% everywhere, and generally to within 0.2%.

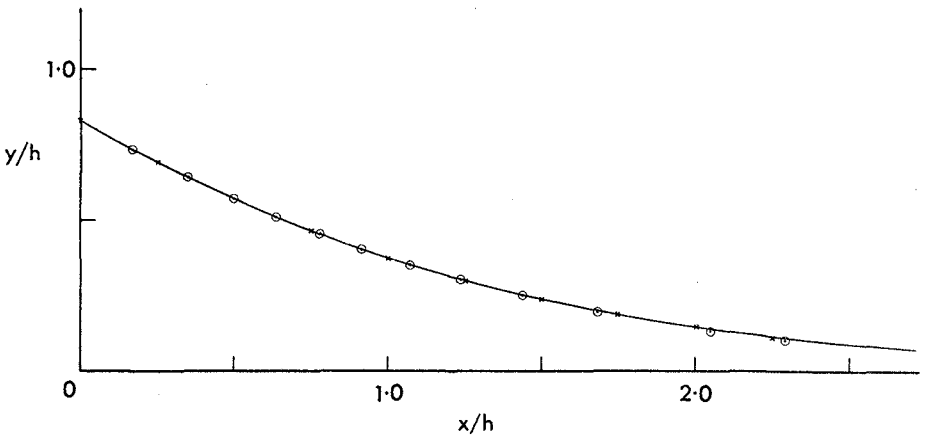


Figure 1. (from Longuet-Higgins, 1974). The profile of the highest solitary wave as given by equation (2.1) (solid line) compared with the numerical calculations of Yamada (1957) (circles) and Lenau (1966) (crosses).

3. SOLITARY WAVES OF ARBITRARY HEIGHT

The properties of solitary waves of arbitrary amplitude a in water of undisturbed depth h have been studied in two recent papers by Longuet-Higgins and Fenton (1974) and by Byatt-Smith and Longuet-Higgins (1976) using quite different methods.

It is convenient to define a parameter ω for the family of solitary waves by the equation

$$\omega = 1 - q^2/gh$$

where q is the particle-speed at the wave crest, in a frame of reference moving along with the phase-speed. For waves of small amplitude, $q \approx \sqrt{gh}$ so ω is small, whereas for limiting waves q vanishes, so $\omega = 1$. In general

$$0 < \omega \leq 1 \tag{3.1}$$

and the complete range of ω is precisely known.

Figure 2 shows a succession of wave profiles, computed precisely for moderate values of ω . The height of the waves increases monotonically with ω . This is in qualitative agreement with the approximate Rayleigh-Boussinesq theory, in which

$$\left. \begin{aligned} y/h &\approx \frac{1}{3} \alpha^2 \operatorname{sech}^2(\frac{1}{2} \alpha x) \\ F^2 &= 1 + \frac{1}{3} \alpha^2 \end{aligned} \right\}$$

and so

$$\omega = 1 - (F^2 - 2a/h) \frac{1}{3} \alpha^2 \approx a/h \tag{3.2}$$

and ω increases almost linearly with a/h . As the wave height increases, so the horizontal width of the profile decreases, like $1/\alpha$ or $(a/h)^{-1/2}$. This implies that successive profiles must intersect each other, and from Figure 2 it is clear that as the amplitude increases, so the point of intersection gradually moves in towards the wave crest.

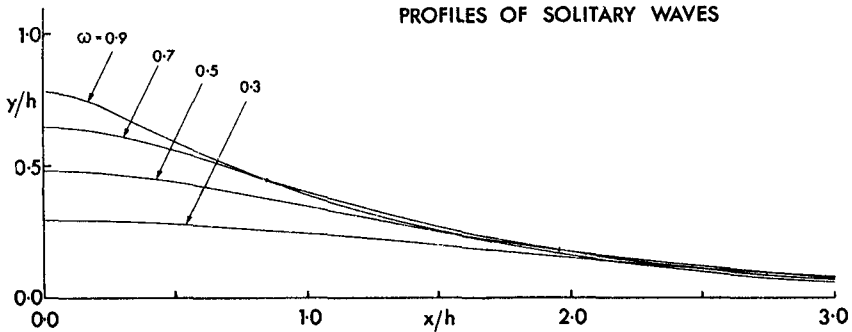


Figure 2. (from Byatt-Smith and Longuet-Higgins, 1976). Profiles of solitary waves at moderate values of the parameter ω .

At finite values of the wave steepness the acceleration near the crest becomes comparable with g and the approximate Rayleigh-Boussinesq theory is no longer valid. An exact theory was however calculated by two methods. In Longuet-Higgins and Fenton (1974) the Rayleigh-Boussinesq theory was treated as the first term in an infinite series in powers of ω , which was carried to high order and then summed by rational approximants (Padé sums). All integral properties converged, up to and including $\omega = 1$, and from these it was possible to calculate also the dimensionless phase-speed F .

Figure 3 shows the dimensionless phase-speed calculated by means of Padé sums, and plotted as a function of the wave steepness a/h . After increasing steadily with a/h , F reaches a maximum and then actually decreases at higher values of a/h . The maximum speed $F = 1.294$ occurs when $a/h = 0.790$, whereas the speed of the highest wave is only $F = 1.286$.

The presence of a maximum in the phase-speed is at first sight surprising, since it implies that over a certain range of steepnesses there can exist two distinct solitary waves in the same depth of water, having the same phase-speed. The reason becomes

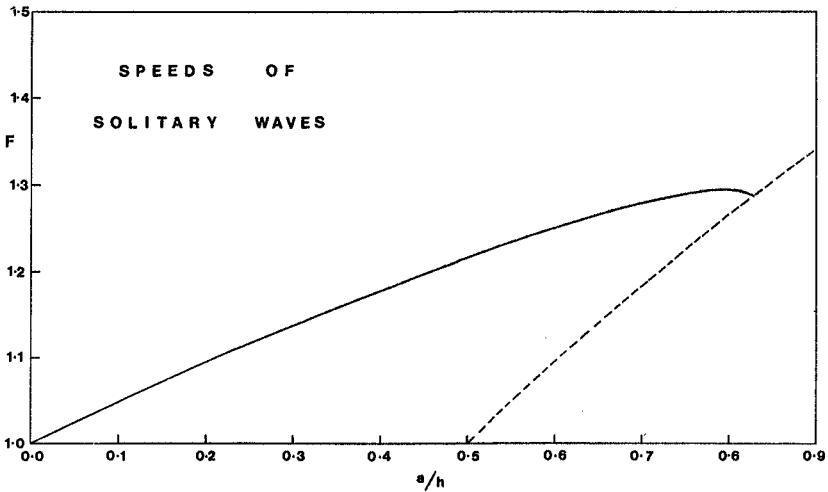


Figure 3. The dimensionless phase-speed $F = c/\sqrt{gh}$ for solitary waves, as a function of the relative crest height a/h .

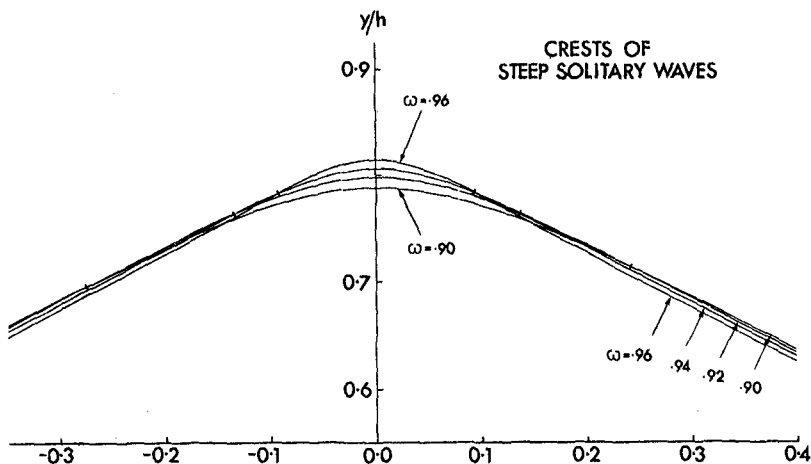


Figure 4. (from Byatt-Smith and Longuet-Higgins, 1976). The form of steep solitary waves close to the wave crest.

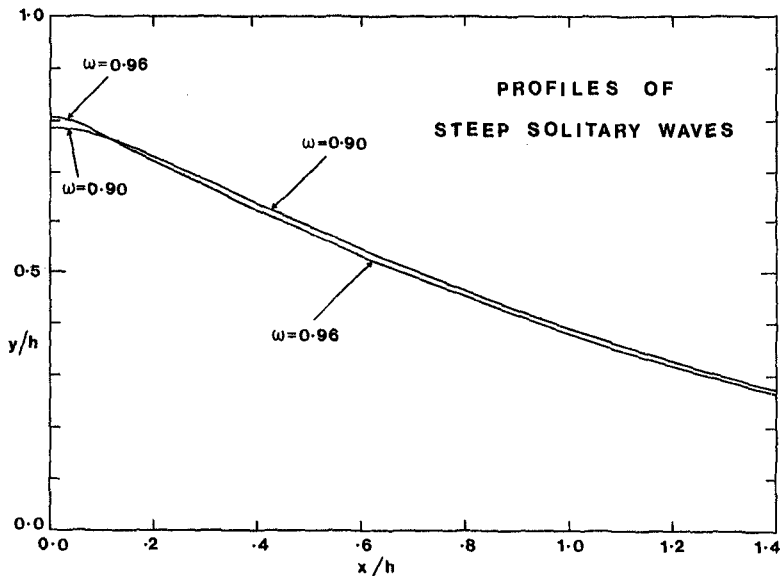


Figure 5. Comparison of the profiles of two steep solitary waves ($\omega = 0.90$ and 0.96).

apparent from Figure 4. This shows some accurately calculated profiles near the wave crest, from $\omega = 0.90$ to $\omega = 0.96$. Evidently the trend begun at the lower wave amplitudes in Figure 2 continues, and as ω increases the point of intersection moves up close to the wave crest. The situation is shown more clearly in Figure 5, from which it will be seen that the higher of the two waves, corresponding to $\omega = 0.96$ actually lies below the lower wave ($\omega = 0.90$) over most of the wave profile. This implies that the average elevation of the higher wave is actually less than that of the lower wave.

Now Starr's exact relation (2.5) can be written in the form

$$(F^2 - 1) = \frac{3}{2} \bar{y}/h \quad (3.3)$$

where \bar{y} is the average surface elevation, defined by

$$\bar{y} = \frac{\int_{-\infty}^{\infty} y^2 dx}{\int_{-\infty}^{\infty} y dx} \quad (3.4)$$

So if \bar{y} decreases as ω increases, so also must F decrease, by equation (3.2).

Although the completeness of the Rayleigh series was questioned by Witting (1975), nevertheless the existence of the maximum speed has been confirmed by a quite different method of calculation based on the integral equation of Byatt-Smith (1970) for solitary waves. In his first paper, Byatt-Smith took the phase-speed F as an independent parameter in the integral equation, and from it calculated the wave height and profile. He was unable to obtain solutions with F greater than about 1.294, and in this neighbourhood convergence was slow. The explanation is apparently that in this neighbourhood a small change in F corresponds to a large change in the profile. But in a second paper (Byatt-Smith and Longuet-Higgins, 1976) ω was taken as independent parameter, and the wave speed F as dependent variable. The solutions converged rapidly and the maximum in F was verified (see Figure 6).

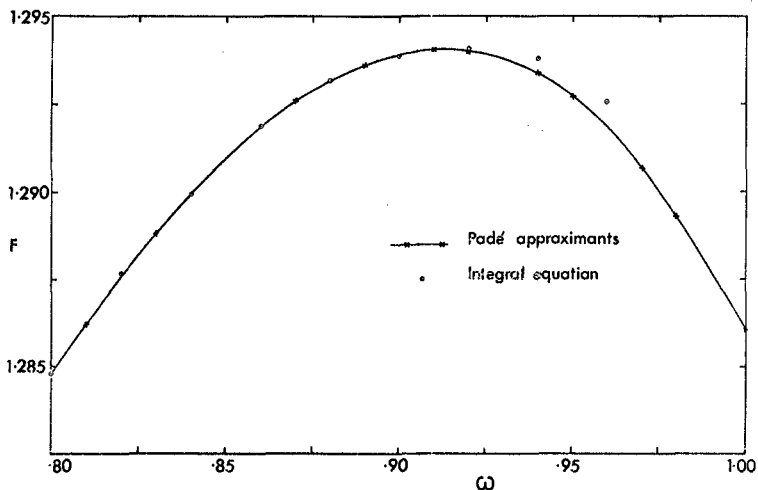


Figure 6. (from Byatt-Smith and Longuet-Higgins, 1976). The dimensionless phase-speed F at high values of ω , calculated by two different methods.

4. WAVES ENTERING SHALLOW WATER

In addition to the maximum in the phase-speed, Longuet-Higgins and Fenton (1974) also found maxima in the mass, momentum and energy of solitary waves, as a function of a/h or of ω (see Figure 7). This has implications for waves entering gradually shoaling water. For, in the absence of appreciable dissipation, the energy E_1 of a solitary wave might be expected to remain a constant. As the mean depth h diminished, the dimensionless energy $E = E_1/\rho gh^2$ would be expected to increase, at first. So, provided the wave remained symmetrical it would be represented by a point travelling up the curve in Figure 7, with both E and a/h increasing.

Before the maximum value of E is reached, however, the wave must leave the energy curve, which it generally does by becoming unsymmetrical and then spilling or plunging forwards (see Section 8). If it plunges heavily, it becomes radically altered. But if it spills gently, it may thereby dissipate enough energy to travel on down the curve more or less as a symmetric wave damped by a whitecap on the forward face. This

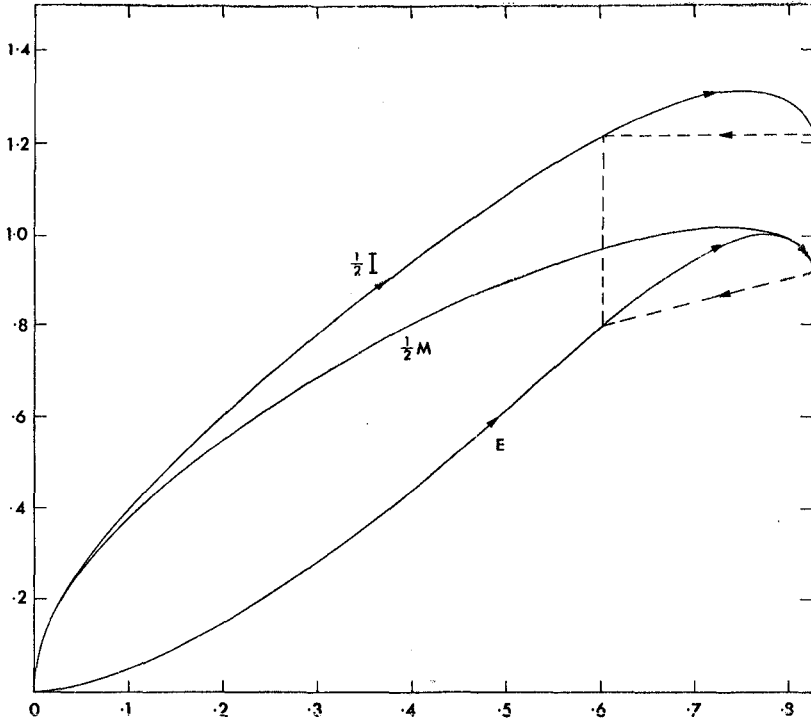


Figure 7. (from Longuet-Higgins and Fenton, 1974). The normalised mass M , momentum I and energy E of a solitary wave, as a function of the relative height a/h .

presumably is a spilling breaker, for which a theory has recently been given by Longuet-Higgins and Turner (1974). In their model, the whitecap was represented as a gravity-current, of density ρ' less than unity, riding down the forward face of an irrotational wave and exchanging mass and momentum by entrainment across the interface. Calculations showed that the flow could exist provided that ρ'/ρ was of order 0.7 (similar to the ratio observed in hydraulic jumps) and that the surface slope exceeded an angle of about 20° .

In this model, however, and also according to observation, the length of the whitecap tends to increase continually*, so producing a disproportionate damping of the wave. What happens when the point in Figure 7 reaches the right-hand edge of the graph, representing the steepest symmetric wave? Longuet-Higgins and Fenton (1974) suggested that it may jump back to a point lower down the curve, representing a wave with almost the same mass and momentum, but with a slightly lower energy. This wave would have a rounded crest and a lower value of a/h . The process might then be repeated.

Some support for this suggestion comes from an analysis of the film of shoaling solitary waves made by Kjeldsen and Olsen (1974). Measurements of the length ℓ of the whitecap as a function of the time t (see Figure 8) show that it increases not continuously but in a series of jumps. At each jump, the crest becomes rounded and a part of the whitecap is lost by being left behind the travelling crest. The remnant appears on the near face of the wave as a patch of aerated water, which quickly subsides.

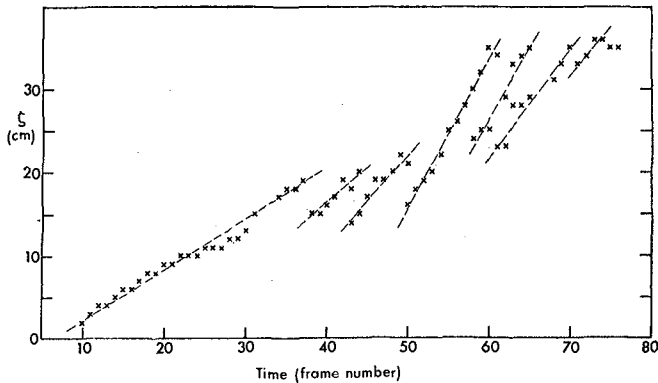


Figure 8. (from Longuet-Higgins and Turner, 1974). Measurements of the length ℓ of the whitecap on shoaling solitary waves as a function of the time, showing intermittency.

*No allowance was made in this model for loss of buoyancy by air bubbles rising through the upper surface.

5. PERIODIC WAVES

For progressive waves in deep water, it has been shown by Schwartz (1974) that the well-known Stokes expansion in powers of the first harmonic a_1 , which is satisfactory at low wave amplitudes, fails to converge at larger wave amplitudes, short of the highest. This is because the waves become markedly non-sinusoidal, developing narrow crests and broad troughs, and the amplitude a_1 of the first harmonic in fact reaches a maximum and then diminishes before the highest wave is reached. So for steepnesses greater than about 0.1 even the higher-order Stokes expansions are divergent and misleading.

Schwartz (1974) overcame this difficulty by using as expansion parameter the wave steepness H/L itself, which increases monotonically throughout the range of possible waves. However, the limiting value of H/L is not accurately known a priori. As an alternative Longuet-Higgins (1975) used the parameter

$$\omega = 1 - \frac{q^2 q'^2}{c^2 c_0^2} \tag{5.1}$$

where q and q' denote the particle speeds at the crest and trough, in a frame moving with the wave, and where c and c_0 are the wave speed and the speed of infinitesimal waves respectively. This parameter is similar to (3.1) and indeed reduces to (3.1) when the depth is finite and the wavelength infinite. The range of ω is from 0 to 1, the value 1 corresponding precisely to the highest wave.

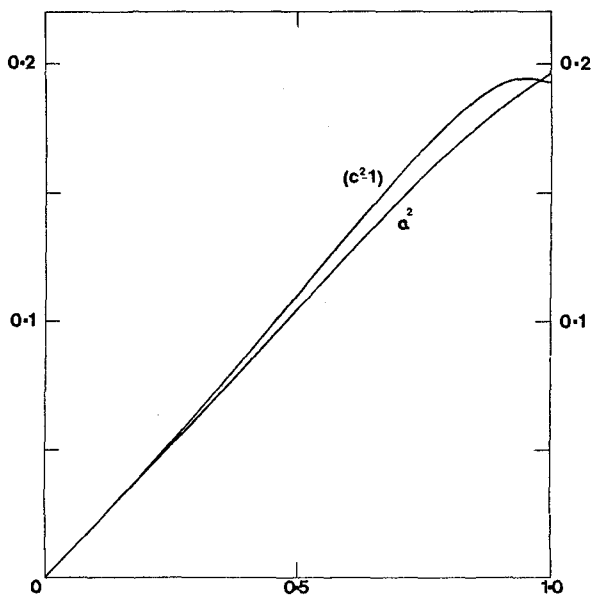


Figure 9. (from Longuet-Higgins, 1975). The square of the wave amplitude a and wave speed c for progressive waves in deep water, as a function of the parameter ω (equation 5.1). The units are chosen so that $g = 1$ and the wavelength $L = 2\pi$. The wave steepness H/L equals a/π .

is the length

$$\ell = q^2/2g \tag{6.1}$$

where q denotes the particle speed at the crest in the frame moving with the wave. Comparison with equation (3.1) shows that ℓ is directly related to ω by

$$\ell = \frac{1}{2}h(1 - \omega). \tag{6.2}$$

As a test of the conjecture, Figure 10 shows the same wave profiles as in Figure 5 ($\omega = 0.90$ to 0.94) now drawn on the new scale ℓ . When ω approaches 1 they do indeed tend to fall along the same curve.

To define our limiting flow we may take radial coordinates (r, θ) with the origin O at a distance $\ell = q^2/2g$ above the wave crest, and with the line $\theta = 0$ vertically downwards. The Bernoulli condition at the free surface is then

$$\left| \frac{dX}{dz} \right|^2 = 2gr \cos \theta \tag{6.3}$$

where $X = \phi + i\psi$ is the complex velocity potential and $z = re^{i\theta}$. We require a solution which, as $r/\ell \rightarrow \infty$, tends to the Stokes corner-flow:

$$X \rightarrow \frac{2}{3} g^{1/2} z^{3/2} \quad \text{as } r \rightarrow \infty, \quad |\theta| \leq \frac{\pi}{3}. \tag{6.4}$$

This problem has been solved numerically in a recent paper by Longuet-Higgins and Fox (1976). The resulting profile is shown in Figure 11 (and also by the broken line in Figure 10). Not unreasonably, the free surface crosses its asymptote at about $r/\ell = 3.32$ and then approaches it very gradually from the outside. It can be shown analytically that for large values of r/ℓ the normal displacement n of the surface from the straight-line asymptote must have the form

$$n/\ell \sim K(\ell/r)^{1/2} \cos [(3\mu/2) \ln r - \epsilon] \tag{6.5}$$

where K and ϵ are amplitude and phase constants and μ is the positive root of the equation

$$\frac{\mu\pi}{2} \tanh \frac{\mu\pi}{2} = \frac{\pi}{24\sqrt{3}} \tag{6.6}$$

In fact $K = 0.60$, $\epsilon = 0.47$ and $\mu = 0.714$. This means that the free surface approaches its asymptote in a very slowly damped oscillation. There is a second crossing of the asymptote at $r/\ell = 68.5$, a third at $r/\ell = 1286$, and so on.

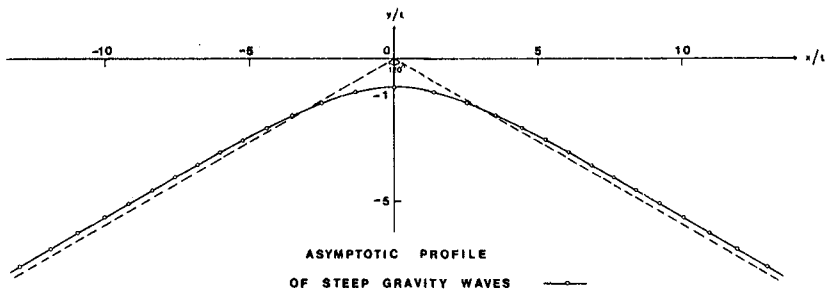


Figure 11. (from Longuet-Higgins and Fox, 1976a). The asymptotic profile of the crests of a steep gravity wave, on a scale $\ell = q^2/2g$.

The results can be checked not only by a direct comparison with the profiles of wave crests calculated independently (such as in Figure 10) but also by a consideration of the maximum surface slope. From Figure 11 it will be seen that between the two crossings of the asymptote at $r/l = 3.32$ and $r/l = 68.5$ the maximum angle of slope must slightly exceed 30° . The actual value is 30.37° . This should correspond to the maximum slope of almost-limiting gravity waves.

Now independent calculations of the complete profiles of steep solitary waves have been made both by Sasaki and Murakami (1973) and by Byatt-Smith and Longuet-Higgins (1976). Their values for the maximum surface slope are plotted against ω in Figure 12. It can be seen that a linear extrapolation of the plotted points passes very close to the asymptotic value that we have obtained independently.

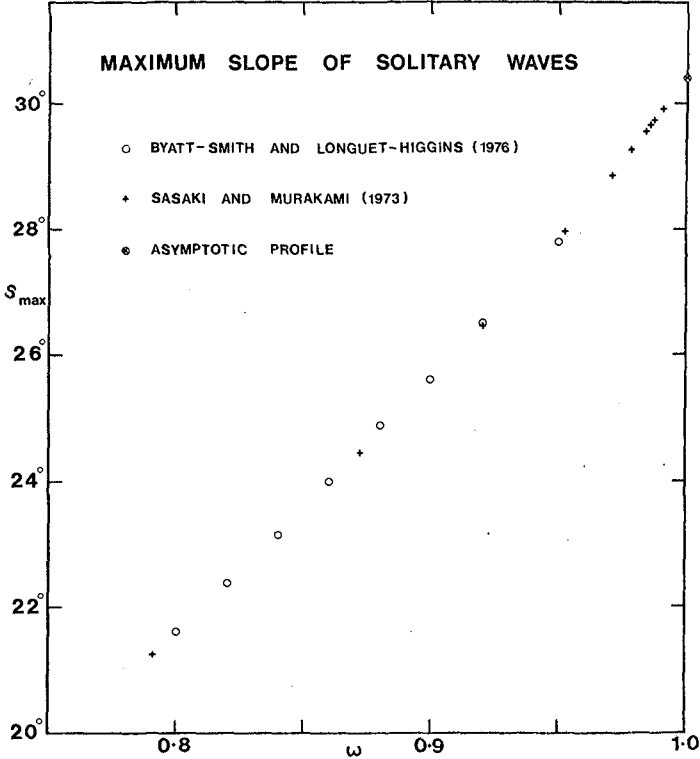


Figure 12. (from Longuet-Higgins and Fox, 1976). The maximum surface slope of steep solitary waves, as a function of the parameter ω . The limiting value at $\omega = 1$ corresponds to the profile of Figure 11.

Figure 13 shows a similar comparison for periodic waves in deep water. The agreement is again very close.

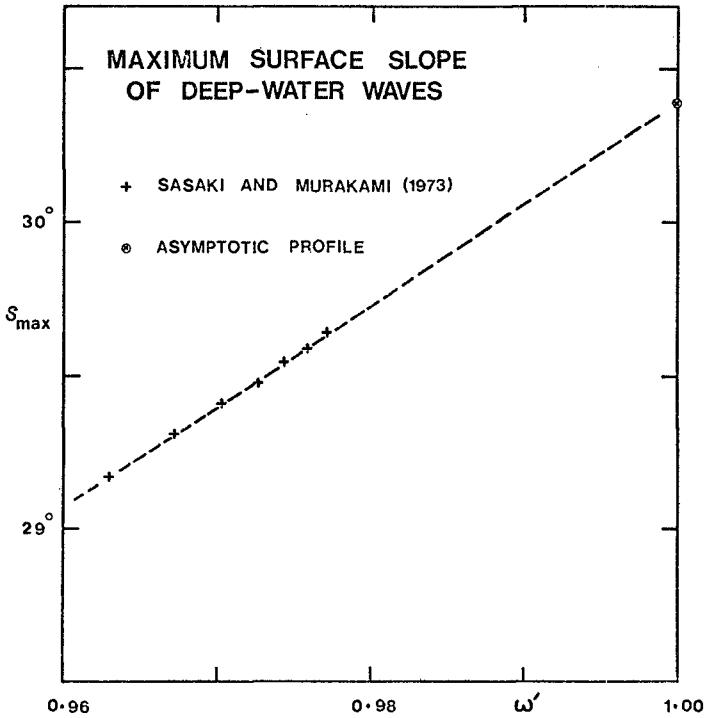


Figure 13. (from Longuet-Higgins and Fox, 1976). The maximum surface slope of progressive waves in deep water, as a function of the parameter ω' .

The acceleration of a fluid particle at the wave crest is given by

$$\ddot{y} = -q^2/R$$

where R is the radius of curvature. From the present profile this is found to be $0.39 g$. In the far-field, as $r/l \rightarrow \infty$, the acceleration tends to the value $\frac{1}{2} g$ directed radially outwards, as in the Stokes corner-flow.

7. IMPROVEMENT IN THE CALCULATION OF STEEP GRAVITY WAVES

The maximum slope will in theory exceed 30° only for very steep, symmetric waves and in a limited region near the crest, which may be affected by instabilities, wind pressures and surface tension. Nevertheless the asymptotic solution found in Section 6 may have practical uses. At present the only accurate calculations of steep, symmetric gravity waves have been obtained by mathematical tour-de-force, either by carrying small-amplitude expansions to very high order or by numerical techniques, such as Fourier series or integral equations, which involve lengthy and complicated numerical schemes. The main value of the asymptotic solution just described is that it may be used as an inner solution, valid near the wave crest, and matched asymptotically to an outer solution representing the flow in the remainder of the wave.

The appropriate matching has already been carried out for periodic waves in deep water by the present author and M.J.H. Fox (1976). As a sample of their results, Figure 14 shows a comparison of the square of the wave speed c^2 plotted against the wave steepness. The peculiar shape of the top of the velocity curve is accurately checked, showing that it is certainly not due to some quirk of the Padé approximants.

Such an approach thus promises to simplify our calculations of steep, symmetric waves, and to improve our understanding of them.

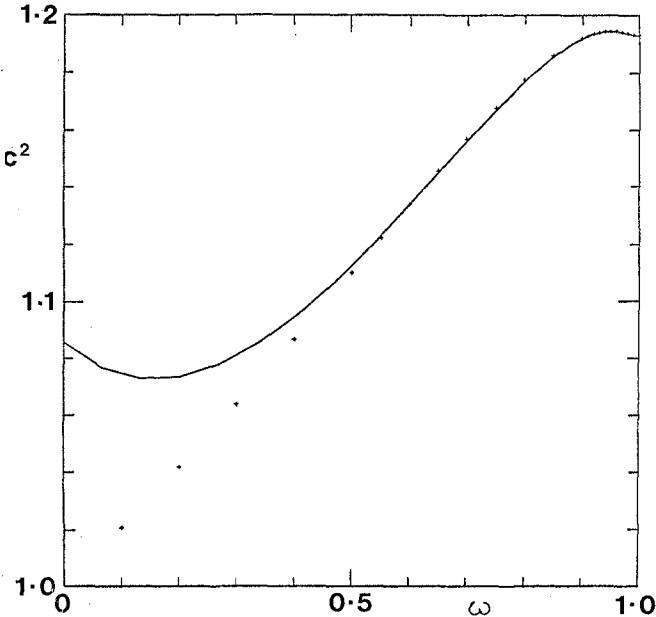


Figure 14. Square of the velocity c for progressive waves in deep water, as a function of ω . The plotted points correspond to the values obtained from Padé sums (Longuet-Higgins, 1975; see also Figure 9). The curve is found independently by matching the asymptotic solution in Section 6.

8. A METHOD FOR CALCULATING UNSTEADY SURFACE WAVES

In natural conditions the occurrence of a steady, steep wave is somewhat exceptional. Even symmetric waves tend to become unsteady and asymmetric long before their energy reaches the theoretical maximum. However, a new and general method for calculating the development of an unsteady wave has recently been given by Longuet-Higgins and Cokelet (1976). So far it has been applied only to waves in deep water but it could readily be extended to waves in water of finite depth.

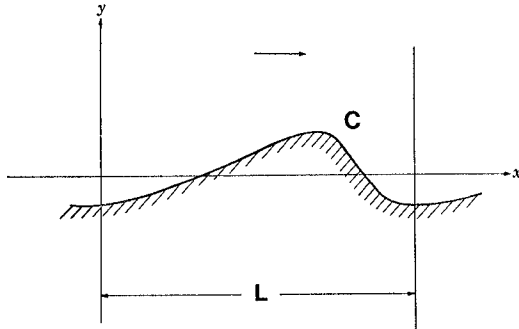


Figure 15. Axes and notation for space-periodic waves in deep water.

The motion is assumed to be irrotational and periodic in space (see Figure 15) though not generally periodic in time. All calculations are carried out with the surface values of the space coordinates (x, y) and of the velocity potential ϕ . For the rates of change of these quantities one has

$$\begin{aligned} \frac{Dx}{Dt} &= \frac{\partial \phi}{\partial x} \\ \frac{Dy}{Dt} &= \frac{\partial \phi}{\partial y} \end{aligned} \tag{8.1}$$

$$\frac{D\phi}{Dt} = -p - gy + \frac{1}{2}(\nabla\phi)^2$$

where D/Dt denotes differentiation following the motion. The last equation follows from the time-dependent Bernoulli equation and the fact that $D\phi/Dt = \partial\phi/\partial t + (\nabla\phi)^2$. Hence, given the surface values of x, y, ϕ and $\nabla\phi$ at some instant t on the surface $C(t)$ one can calculate x, y and ϕ at time $(t + dt)$ on the displaced surface $C(t + dt)$.

To proceed to the next time-step we need to know both components of the velocity on $C(t + dt)$. We can obtain the tangential component $\partial\phi/\partial s$ immediately, by differentiating $\phi(t + dt)$ along the new surface. However we still lack the normal component of velocity $\partial\phi/\partial n$ on $C(t + dt)$.

Now because of the space-periodicity we can transform C into a closed contour C' (Figure 16) simply by writing

$$e^{ik(x + iy)} = \zeta, \quad (k = 2\pi/L). \tag{8.2}$$

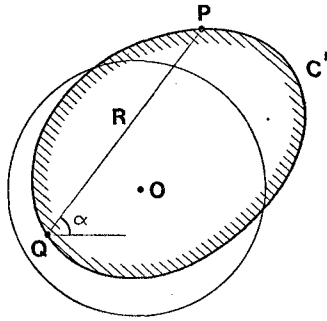


Figure 16. One wavelength in the (x, y) plane transformed to a closed domain in the z -plane.

The domain of the fluid goes into the interior of C' and the points at infinite depth go into the origin $z = 0$. We then have to solve, in effect, the well-known Dirichlet problem, namely to find $\partial\phi/\partial n$ on a contour C' , given ϕ on C' and

$$\nabla^2\phi = 0 \quad (8.3)$$

everywhere inside C' .

This problem can be solved as follows (see Figure 16). Let (R, α) denote the polar coordinates of a running point P on the boundary, relative to a fixed point Q , also on C' . Then it follows from Green's theorem that

$$\int_{C'} \frac{\partial\phi}{\partial n} \ln R \, ds = \pi\phi_Q + \int_{C'} \phi_P \, d\alpha \quad (8.4)$$

where in the right-hand integral we take the principle value. Since ϕ is known everywhere on C' , the right-hand side is given, and equation (8.4) is then a linear integral equation for $\partial\phi/\partial n$, with given kernel $\ln R$. Solution of this equation gives us $\partial\phi/\partial n$ on $C(t + dt)$, and the time-stepping can proceed.

Numerical solution of equation (8.4) has been carried out by Longuet-Higgins and Cokelet (1976) replacing the boundary by a finite number N of integration points. Typically $N = 60$ for one wavelength. Details of the method, which are vital for its accuracy and success, are given in their paper. The method was first tested for accuracy on a free symmetric wave of finite amplitude for which the form and phase-velocity were calculated independently by the method of Section 5, and good agreement was obtained. Then the following experiment was performed. As initial state was chosen a progressive wave of fairly large amplitude, whose energy was 0.80 times the maximum E_{\max} for a steady symmetric wave of that wavelength. The energy was then raised by applying to the surface (numerically) a pressure of the form

$$p = \left\{ \begin{array}{l} p_0 \sin(kx - \sigma t) \sin \sigma t, \quad (0 < \sigma t < \pi) \\ 0 \quad (\sigma t < 0 \text{ and } \sigma t > \pi) \end{array} \right\} \quad (8.5)$$

through the boundary-conditions (8.1). This represented a sinusoidal distribution of pressure, in quadrature with the fundamental harmonic of the surface elevation, increasing and dying away smoothly over half a wave period (π/σ). After the surface pressure had fallen to zero, the wave was supersaturated, that is its level exceeded E_{\max} . It was then allowed to run free. Its subsequent development can be followed in Figure 17.

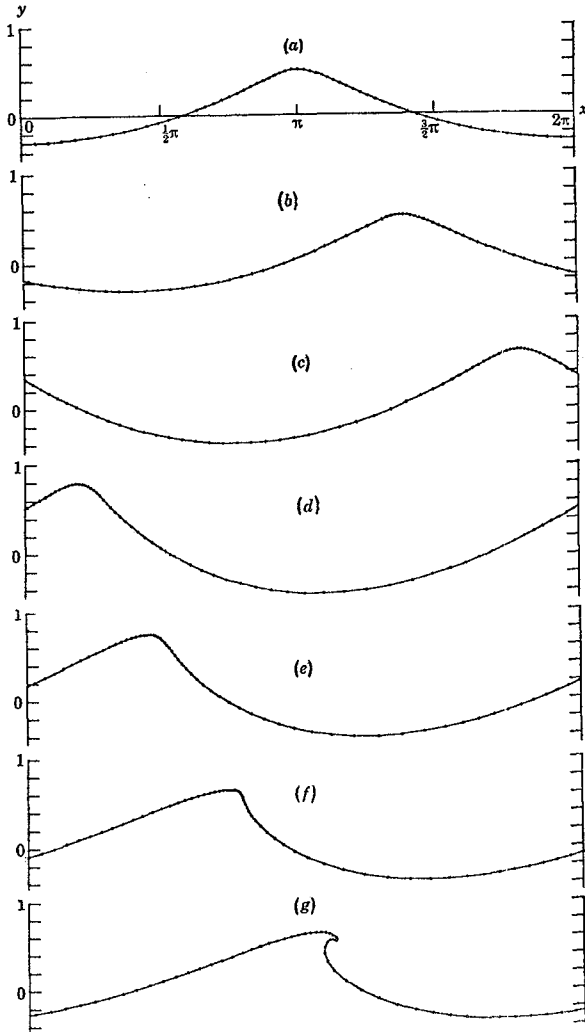


Figure 17. (from Longuet-Higgins and Cokelet, 1976). Development of a progressive wave in deep water. From (a) to (c) a surface pressure (8.5) is applied to the rear face of the wave. From (d) to (e) the wave is free.

Figure 18 gives a close-up view of the free surface near the instant of overturning. The figure shows successive positions of the free surface (actually every 3 time-steps) in a frame moving with the speed c_0 of infinitesimal waves. The plotted points refer always to the same marked particles, so that a line through a succession of points defines a particle trajectory, in this reference frame.

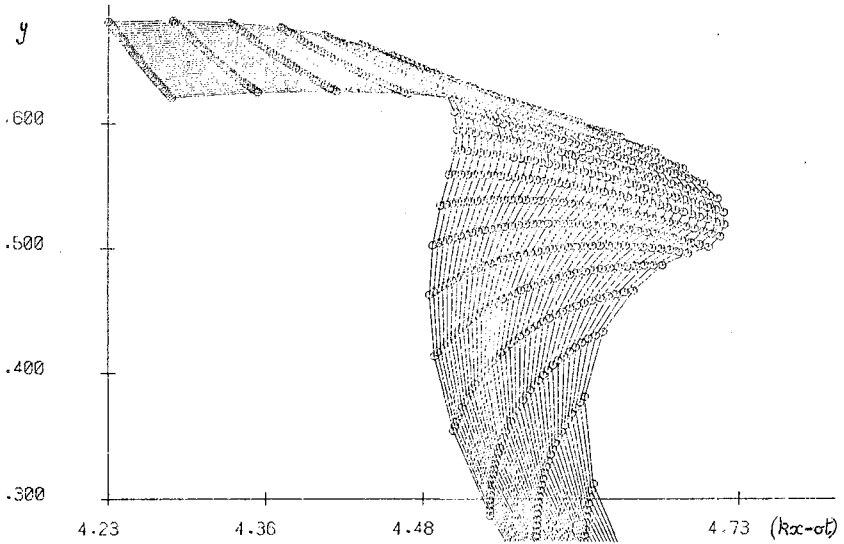


Figure 18. (from Longuet-Higgins and Cokelet, 1976). Successive profiles of the free surface near the instant of overturning, seen in a reference frame moving with speed c_0 .

The particles have a welcome tendency to congregate near points of high surface curvature, which is precisely where they are needed for computational accuracy.

It will be seen that the crest remains rounded until well past the instant when the surface becomes vertical. Thereafter the curvature near the tip of the breaker increases rapidly. The free surface can be followed by this method only so long as the separation between adjacent particles does not exceed a fraction of the local radius of curvature. The question whether the curvature becomes infinite in finite time cannot be decided by this method.

In practice the tip of the jet will be much influenced both by surface tension, which we have neglected, and by air currents. Both these may cause it to break up into spray. Both effects could possibly be included in the calculation. The present calculations were intended to apply only to waves on a sufficiently large scale.

Though the computation involves only the surface values of x , y and ϕ , the pressure and velocity components in the interior may also be found from the surface values, by the use of Cauchy's theorem. The pressure gradients in the tip are small, but there is no evidence of a reversed normal gradient of the pressure.

Because it uses the velocity potential ϕ yet follows marked particles, the above technique may be called MEL (mixed Eulerian and Lagrangian). The example just discussed illustrates only one possible application of the general method. Various other initial conditions might be chosen so as to correspond, for example, to a standing wave, or to a partially reflected wave, or to a mixture of progressive wave trains having rationally related wavelengths. These would constitute a wave group with slowly varying wave envelope. It will be of interest to see how the resulting energy and momentum lost in the jet of the breaking wave are related to the different initial conditions.

9. EXPERIMENTAL CONFIRMATION

Although the above computations were for deep water, nevertheless one would expect the local behaviour of the wave crest to be asymptotically similar whether in deep or shallow water. To test whether the surface could remain smooth and continuous after the tangent became vertical, the author and N.D. Smith, with the collaboration of Dr. N. Hogben, made a high-speed film of waves breaking on a 1:6 beach slope, in the No. 2 Towing Tank of the National Physical Laboratory at Teddington. Figure 19 shows one frame from a film taken at 500 frames/sec. The grid-spacing is 5.0 cm. The film confirms that the free surface can indeed remain smooth and rounded until after overturning takes place.

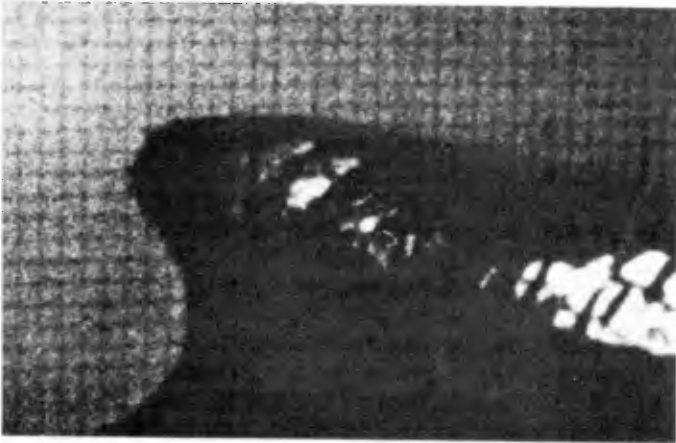


Figure 19. Wave breaking on plane beach, slope 1:6.

REFERENCES

- Byatt-Smith, J.G.B. 1970 An exact integral equation for steady surface waves.
Proc. Roy. Soc. Lond. A. 315, 405-418.
- Byatt-Smith, J.G.B. and Longuet-Higgins, M.S. 1976 On the speed and profile of steep solitary waves.
Proc. Roy. Soc. Lond. A. 350, 175-189.
- Cokelet, E.D. 1976 Steep gravity waves in water of arbitrary uniform depth.
(in preparation).
- Fenton, J. 1974 A ninth-order solution for the solitary wave.
J. Fluid Mech. 53, 257-271.
- Kjeldsen, S.P. and Olsen, G.B. 1971 Breaking waves (16mm film).
Tech. Univ. of Denmark, Copenhagen.
- Lamb, H. 1932 Hydrodynamics, 6th ed.
Cambridge Univ. Press.
- Lenau, C.W. 1966 The solitary wave of maximum amplitude.
J. Fluid Mech. 26, 309-320.
- Longuet-Higgins, M.S. 1963 The generation of capillary waves by steep gravity waves.
J. Fluid Mech. 16, 138-159.
- Longuet-Higgins, M.S. 1973 On the form of the highest progressive and standing waves in deep water.
Proc. Roy. Soc. Lond. A. 331, 445-466.
- Longuet-Higgins, M.S. 1974 On the mass, momentum, energy and circulation of a solitary wave.
Proc. Roy. Soc. Lond. A. 337, 1-13.
- Longuet-Higgins, M.S. 1975 Integral properties of periodic gravity waves of finite amplitude.
Proc. Roy. Soc. Lond. A. 342, 157-174.
- Longuet-Higgins, M.S. and Cokelet, E.D. 1976 The deformation of steep surface waves on water. I. A numerical method of computation.
Proc. Roy. Soc. Lond. A. 350, 1-26.
- Longuet-Higgins, M.S. and Fenton, J.D. 1974 On the mass, momentum, energy and circulation of a solitary wave. II.
Proc. Roy. Soc. Lond. A. 340, 471-493.
- Longuet-Higgins, M.S. and Fox, M.J.H. 1976 Theory of the almost highest wave.
(in preparation).
- Longuet-Higgins, M.S. and Turner, J.S. 1974 An "entraining plume" model of a spilling breaker.
J. Fluid Mech. 63, 1-20.
- Sasaki, K. and Murakami, T. 1973 Irrotational, progressive surface gravity waves near the limiting height.
J. Oceanogr. Soc. Japan 22, 94-105.
- Schwartz, L.W. 1974 Computer extension and analytic continuation of Stoke's expansion for gravity waves.
J. Fluid Mech. 62, 553-578.
- Stokes, G.G. 1880 On the theory of oscillatory waves. Appendix B: Considerations relative to the greatest height of oscillatory irrotational waves which can be propagated without change of form.
Math. and Phys. Pap. 1, 225-228.
- Witting, J. 1974 On the highest and other solitary waves.
SIAM J. Appl. Math. 28, 700-719.
- Yamada, H. 1957a Highest waves of permanent type on the surface of deep water.
Rep. Res. Inst. Appl. Mech. Kyushu Univ. 5, 37-52.
- Yamada, H. 1957b On the highest solitary wave.
Rep. Res. Inst. Appl. Mech. Kyushu Univ. 5, 53-67.